

This is the peer reviewed version of the following article:

Experimental Investigation of Shaft Radial Load Effect on Bearing Fault Signatures Detection / Immovilli, Fabio; Cocconcelli, Marco. - In: IEEE TRANSACTIONS ON INDUSTRY APPLICATIONS. - ISSN 0093-9994. - 53:3(2017), pp. 2721-2729. [10.1109/TIA.2016.2633236]

Terms of use:

The terms and conditions for the reuse of this version of the manuscript are specified in the publishing policy. For all terms of use and more information see the publisher's website.

14/05/2024 12:16

(Article begins on next page)

Experimental Investigation of Shaft Radial Load Effect on Bearing Fault Signatures Detection

Fabio Immovilli, *Member, IEEE*, and Marco Cocconcelli

Abstract—This paper investigates the influence of external radial load applied to the shaft on bearing fault detection based on vibration or current in induction motors operating under different conditions. This paper details the results of a laboratory trial comprising different test sets on the condition monitoring and fault diagnostic of a 6-poles induction motor using a design of experiment (DOE) approach. The dedicated test setup comprises a custom-made fixture that allows to dynamically vary the radial load applied to the output shaft. The aim is to investigate the effects of radial load on the fault diagnosis of shaft bearings and the interactions between other operating parameters such as output torque. Specific scalar parameters have been proposed for the condition monitoring of the test motor from vibration and current data. The correct choice of the significant parameters is proven by the strong dependency on the damage returned by DOE results.

Index Terms—Fault diagnosis, Condition monitoring, Induction motors, Ball bearings, Air gaps, Modulation, Frequency domain analysis, Harmonic analysis, Current measurement, Vibration measurement

I. NOMENCLATURE

f_{car} fault characteristic frequency
 F_{be} stator current fault characteristic frequency
 f mains electric supply frequency
 F_r rotor mechanical frequency
 F_{cage} cage fault frequency
 F_{outer} outer raceway fault frequency
 F_{inner} inner raceway fault frequency
 F_{ball} ball fault frequency
 Z number of ball bearing's spheres

II. INTRODUCTION

Electrical and mechanical fault diagnosis in induction machines is an extensively investigated field for cost and maintenance savings, as induction motors operating at mains frequency are still the most widespread rotating electric machines in industry, mainly because of their low price, ruggedness and reliability. Many papers can be found in the literature concerning the general condition monitoring of induction machines [1] - [3]. The distribution of failures within the machine sub-assemblies is reported in many reliability survey papers [4], [5]. A rough classification identifies four classes: bearings faults, stator related faults, rotor related faults, other faults

F. Immovilli is with the Department of Sciences and Methods of Engineering, University of Modena and Reggio Emilia, Reggio Emilia, RE, 42122 Italy e-mail: fabio.immovilli@unimore.it

M. Cocconcelli is with the Department of Sciences and Methods of Engineering, University of Modena and Reggio Emilia, Reggio Emilia, RE, 42122 Italy e-mail: marco.cocconcelli@unimore.it

(lack of cooling, loose terminal box connection). Bearing faults are one of the most common failures in electrical machines especially in the small-medium power sizes [6]. Bearing faults that are not detected in time cause malfunction, loss of performance, reduced efficiency and may even lead to failure of the driven machinery, [7], [8].

In many situations diagnostics methods based on the analysis of the vibration signals have proved their effectiveness [9], [10]. Among the mechanical problems detected by vibration spectra there are: imbalance, misalignment, loose fitting, bent shafts, and bearing localized faults. On-line fault detection can be obtained by vibration analysis, but the diagnosis equipment is costly and invasive, requiring dedicated equipment and specific sensors to be installed.

Motor current signature analysis (MCSA) is an alternative method that relies on the monitoring of electrical quantities, that are already acquired in the final application, e.g. to implement the control of an electric drive, thus do not require the installation of dedicated transducers. Many research activities were focused on the diagnosis of bearing faults by MCSA [11] - [13]. In many cases mechanical signals cannot be directly acquired, e.g. in harsh environments, remote locations, or because the application is difficult to access. Under such conditions, electric signal measurements would be preferable as they are more immune to external disturbances, [14]. Non-invasive fault diagnosis should ideally detects faults at the early stage, to allow for scheduled maintenance, minimizing system downtime. Under this circumstances, fault signature components feature a very small amplitude that is usually buried in noise and can lead to false positive detection [15]. The use of suitable signal processing techniques is required to efficiently extract the fault signatures from raw signals. The use of current and/or voltage signal constitutes a non-invasive method to bring information necessary to diagnose a fault in the system via on-line monitoring of the electric machine [16], [17].

The present work aims at investigating the effects of radial load at the shaft end of the machine on the shaft bearings fault signature detection. This paper details the results of a laboratory trial comprising different test sets on the condition monitoring and fault diagnostic of a 6-poles induction motor using a design of experiment (DOE) approach. In particular, the paper focuses on the diagnostics of ball bearings supporting the drive end shaft of the motor.

Considering realistic installations in the industry, radial forces at the shaft of the motor can vary remarkably both under different mounting and operating conditions. Radial forces at the shaft can be almost zero in case of planetary gearboxes or centrifugal pump applications; on the other hand they can be

very high in case of grooved belt transmissions or industrial vibrators applications. The presence of a relevant radial force produces a defined high contact pressure area between the outer case and the revolving elements of the bearing, that can result in a periodic vibration of the shaft. Results in literature suggest that this condition can in turn lead to false positive detection in bearing diagnostics even in case of vibration based condition monitoring [18].

The effect can be explained by analyzing radial force transmission among the bearing components: the radial load acts on the shaft that is supported to the stator by the rolling bearings. In particular the radial load is transmitted from the inner raceway of the bearing, to the rolling elements, than to the outer raceway fixed on the stator (see Fig.1 for a description of the bearing elements). Under working conditions the inner raceway is rotating at the shaft speed, the rolling elements are advancing at the cage speed (Eq. 2), while the outer raceway is fixed. Indeed, only a fraction of the rolling elements supports the radial load, specifically those which are passing through the radial load zone. The exact number oscillates between a minimum and a maximum value, since the rolling elements are moving and a new element continuously enters the load zone while another one exits. This causes a fluctuation of the bearing's radial stiffness, with a periodicity that has the same frequency of the outer race characteristic frequency (Eq. 3), a detailed model was presented in [14].

The paper contribution is to experimentally investigate the effects and the interactions of a radial load at the shaft end on the diagnostics of ball bearings by means of both vibration and current analysis with the motor under test (MUT) operating under different conditions (load torque).

Multivariable problems can be approached following a statistical method. The Design of Experiment (DOE) procedure, a powerful statistical technique based on the analysis of variance (ANOVA), can be conveniently applied to these classes of problems. The DOE is the branch of science that deals with designing the correct sequence of experiments to minimize measurement errors and maximize the evidence of dependencies between causes and results.

In [19] the foundation of the DOE is defined, suggesting methodologies like the comparison between results, randomization of the test, the statistical replication of the experiment, the blocking of experimental units into groups, the orthogonality and the factorial experiment. The latter is efficient at evaluating the effects and possible interactions of several factors on the output. Nowadays several software are available, helping the user to design a correct layout of the experiment, with a selected number of independent inputs and resulting outputs. The inputs to the system are called "factors" and each of them could have more than one value (usually called "levels"). The number of factors and the number of levels determine the complexity of the experimental plan and the total number of tests to be done.

The paper is organized as follows: section III reviews the relationship between vibration and current components presented in literature. Section IV outlines the proposed fault indexes to be used in the Design of Experiment analysis. Section V and VI presents the experimental setup and the

factorial design of experiment respectively. Section VII reports the results for test runs at different working conditions and bearing damage, followed by conclusion and final remarks.

III. VIBRATIONS AND CURRENTS BASED CONDITION MONITORING

As previously seen, numerous papers in literature deal with the detection and diagnosis of electrical and mechanical faults based on MCSA in induction motors [20], [21]. The link between vibrations and motor current spectral components is still under investigation in the scientific community and is treated in literature according to different approaches.

The first approach links the vibration component to a torque ripple that produces a speed ripple on the electric machine [22]. Hence the vibration is seen as a torque component that generates in the current a chain of components at frequencies F_{be} :

$$F_{be} = | f \pm k f_{car} | \quad (1)$$

where k is an integer.

According to the second approach, the vibration component causes a rotor eccentricity [23]. A unifying approach is presented in [24].

In all cases, vibrations introduce modulation in the stator currents at frequencies F_{be} related to the mechanical frequencies and electrical supply frequency, Eq. (1).

Radial bearings consist of two concentric rings containing inner and outer races, separated by rolling elements, Fig. 1. Rolling elements are separated by a cage: a component that maintains a constant angular pitch between adjacent rolling elements, preventing contacts.

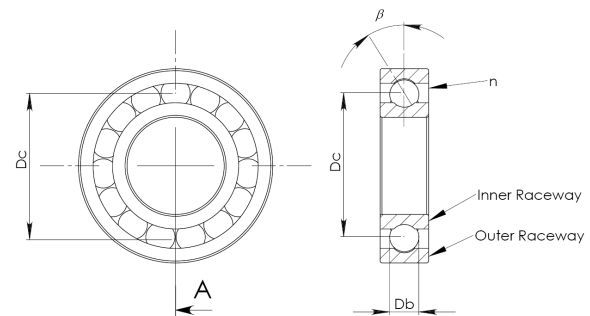


Fig. 1. Bearing structure and characteristic dimensions.

Localized faults will produce characteristic vibration frequency components. These bearing fault frequencies are a function of the bearing geometry and the relative speed of the outer and the inner ring. Characteristic vibration frequencies can be calculated from the bearing's physical dimensions, Fig. 1. In particular, considering the outer ring fixed to the frame:

$$F_{cage} = \frac{1}{2} F_r \left(1 - \frac{D_b \cos \beta}{D_c} \right) \quad (2)$$

$$F_{outer} = \frac{n}{2} F_r \left(1 - \frac{D_b \cos \beta}{D_c} \right) \quad (3)$$

$$F_{inner} = \frac{n}{2} F_r \left(1 + \frac{D_b \cos \beta}{D_c} \right) \quad (4)$$

TABLE I
VIBRATION RELATED COMPONENTS IN THE STATOR CURRENT SPECTRUM.

	Model based on torque fluctuations
Outer raceway defect	$f \pm k F_{outer}$
Inner raceway defect	$f \pm k F_{inner}$
Ball defect	$f \pm k F_{ball}$
Cage defect	$f \pm k F_{cage}$

$$F_{ball} = \frac{D_c}{D_b} F_r \left[1 - \left(\frac{D_b \cos \beta}{D_c} \right)^2 \right] \quad (5)$$

where D_b stands for the ball diameter, D_c for the pitch diameter, n for the number of rolling elements, β for the ball contact angle, Fig.1. Table I summarizes the corresponding vibration related components on the machine current for the torque fluctuation model.

Considering the torque ripple model, vibration effects on machine currents are caused by small speed fluctuations of the rotor. Because of electromechanical filtering effects (due to the rotor inertia and winding inductance) MCSA is more sensitive to low frequency phenomena [25].

In summary, it is usually very difficult to retrieve bearing fault signature components by MCSA. Especially because when dealing with realistic incipient faults, the fault signature is buried in noise or is a small fraction of the fundamental supply current, especially when operating at rated load. In [25] the torque ripple associated with a realistic (not drilled) localized fault was experimentally measured on a machine of similar size: the peak value of the torque ripple was measured to be 6 mNm , corresponding to a current ripple referred to the active current amplitude of 0.2–0.5 mA . Such harmonic components are 3-4 orders of magnitude smaller than the nominal current of the machine, lying near the accuracy class of common industrial current transducers. The aim of this paper is to investigate the influence of the working conditions of the motor on two scalar indicators used for condition monitoring of the bearing. In particular the working conditions comprise the radial load, the torque applied at the motor shaft and the bearing condition.

In the following paragraphs, the proposed scalar indicators for two test sets are presented and a factorial design of experiment is detailed to assess the sensitivity of the indicators. Finally the results obtained on dedicated test bench are presented and discussed.

IV. SIGNAL PROCESSING AND PROPOSED FAULT INDEXES

Usually vibration and current signals are processed in order to detect fault signature data: a short outline of the most common signal processing techniques used for fault detection is reported hereafter. Statistical scalar indicators are used to provide a single parameter representative of the health status of the electro-mechanical system being monitored. Usually the quantity of interest is the vibration signal and the most commonly used indicators are the Root Mean Square value (RMS) of the vibration velocity and the Kurtosis [26]. The

TABLE II
SPECIFICATIONS OF THE BALL BEARING USED IN THE EXPERIMENTS

Inner diameter	25	[mm]
Outer diameter	52	[mm]
Number of spheres	9	
Basic static load rating	7800	[N]
F_{inner}/F_r	5.41	
F_{outer}/F_r	3.585	
F_{cage}/F_r	0.398	
F_{ball}/F_r	4.715	

RMS value is closely related of the energy lost due to dissipative phenomena: indicative RMS thresholds are suggested in [27] and [28].

The Kurtosis can be seen as the deviation from the standard probability distribution of a real-valued random variable. In case of a healthy bearing, white noise is expected with a normal Gaussian distribution. A fault introduces specific components that depart from the normal distribution, thus increasing Kurtosis value [29]. More refined statistical approach and feature extraction algorithms are also employed, especially for fault classification purposes [30].

Frequency domain analysis is the most important technique used so far in literature [26]. Usually a fault on a moving element modulates the amplitude of vibration signal with a frequency which is characteristic of the damage [31], [32]. Envelope analysis can be used to effectively retrieve the fault signature components, e.g. Hilbert transform via the *analytical signal*, which is a generalization of the phasor concept that allows to conveniently separate the effects of amplitude modulation and phase modulation.

In the last decade Randall and Antoni [33], [34] proposed that the vibration signal from a faulty bearing is a second-order cyclostationary process. Introduced by Gardner [35], a cyclostationary process can be viewed as multiple interleaved stationary processes, having statistical properties that vary cyclically with time. A second-order statistics cyclostationary process exhibits a cyclic variation of the autocorrelation function. Instead of a simple spectrum, significant results have been reached so far [26] by computing the auto-power-spectrum of the vibration signal. The Wiener-Khinchin theorem states that the autocorrelation function of a wide-sense-stationary random process has a spectral decomposition given by the power spectrum of that process [36].

Because the present paper employs a factorial design of experiment to investigate the effects of the operating conditions on the fault indicators, statistical scalar fault indicators are preferred and will be used to assess the response of the system.

In this paper two scalar fault indexes are proposed for bearing fault detection. Since the working condition of the motor is stationary, a frequency domain analysis is used for the processing of vibration data. In particular the power spectrum of the vibration signal is computed and bandpass filtered in a specific frequency band to better highlight the possible presence of characteristics fault frequencies.

With reference to the characteristics fault frequencies defined in Eqs. 2-5, summarized in Tabs. II and III, the rotational

TABLE III
EXPECTED FAULT FREQUENCIES OF THE BALL BEARING USED IN THE EXPERIMENTS

f	50	Hz
F_r	15.9	Hz
F_{inner}	86.2	Hz
F_{outer}	57.1	Hz
F_{cage}	6.3	Hz
F_{ball}	75.1	Hz

frequency used in the tests, the chosen bandpass frequency band is [50 Hz - 80 Hz]. The frequency span is suitable for both localized defect on the outer race and ball fault damage in case of artificial brinelling. The maximum amplitude of the spectrum in that frequency range is the fundamental fault frequency and is taken as fault index for the vibration analysis. The use of a frequency band instead of the single fault frequencies is intended to simplify the computation of the signature recognition. The selected band is relatively flat and the presence of any fault signature is clearly identified, as confirmed by the experiments in Section VII. Figure 2 shows the post-processing flowchart of the vibration signal.



Fig. 2. Post-processing flowchart of the vibration signal.

The current signal has been filtered by a series of notch filters in order to remove the 50 Hz fundamental mains supply frequency and its higher harmonics over all the frequency range. The Root Mean Square (RMS) value of the filtered current is taken as fault index for the current analysis. The RMS is used to take into account the energy of the residual signal, considering that any damage to the motor requires additional energy, appearing in the spectrum as sideband modulations according to Table I. Since the torque ripple due to the bearing fault impacts is independent of the torque load on the machine [25], the residual signal was chosen as a good candidate for a robust scalar fault index. Figure 3 shows the post-processing flowchart of the current signal. A detailed description of the experimental setup is provided in the next section.



Fig. 3. Post-processing flowchart of the current signal.

V. TEST SETUP

The experimental setup, Fig. 4, comprises the electrical motor under test (MUT) that is installed on a test bench in order to vary both the radial and the torque load conditions. The chosen MUT is a three phase induction machine operated directly connected to the 50 Hz mains grid. The test bench also houses a brake/dynamometer consisting of a vector controlled induction machine in order to vary the load torque on the MUT. Table IV summarizes the nameplate data of the MUT.

TABLE IV
NAMEPLATE DATA OF THE MOTOR UNDER TEST

Nominal Power	1100	[W]
Number of poles	6	
Nominal current	2.8	[A]
Power Factor	0.76	
Nominal Torque	11.5	[Nm]
Stator Resistance	5.65	[Ω]

Radial load on the MUT shaft is provided by a specially designed test fixture, Fig. 5, comprising a pneumatic cylinder coupled to a manifold with pressure regulator and transducer to modulate the radial load. The cylinder is connected to a crosshead carrying an extension shaft that allows to apply a variable radial force at the motor shaft's end.

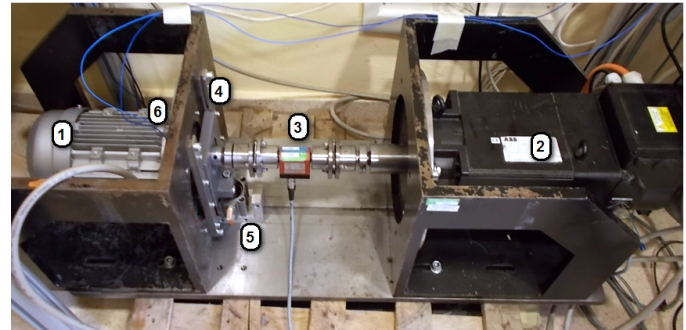


Fig. 4. Test setup overview: (1) MUT; (2) brake/dynamometer; (3) torque meter; (4) crosshead; (5) pneumatic cylinder; (6) accelerometer position. The compressed air hose connecting the cylinder to the manifold with pressure regulator and transducer is not shown.

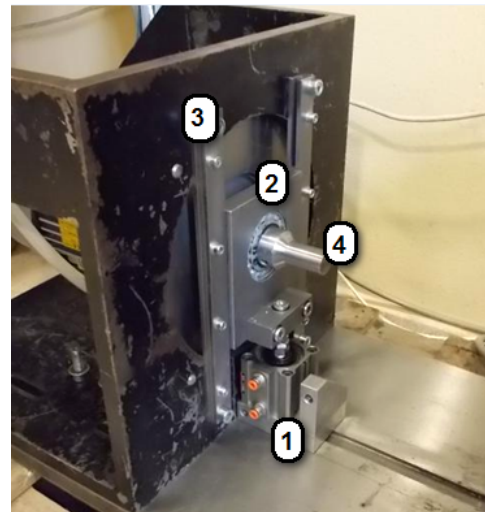


Fig. 5. Test fixture detail: (1) pneumatic cylinder; (2) crosshead assembly; (3) slide guides; (4) extension shaft. The compressed air hose connecting the cylinder to the manifold with pressure regulator and transducer is not shown.

The cylinder is supplied with compressed air at a pressure up to 6 bar, corresponding to a radial force of up to 1180 N exerted on the front bearing.

The test bearing is a SKF 6205 deep groove ball bearing, Tab. II summarizes the characteristic dimensions and fault frequencies supplied by the manufacturer. Table III summarizes

the characteristic fault frequencies with the MUT operated at nominal frequency.

Two different damages were artificially made on the bearings, in order to apply DOE to different data test set:

- a single defect on the outer raceway, created by chemical etching of the bearing outer race, Fig. 6-left.
- a simulated brinelling defect, generated applying a mechanical load of 4 tons (40 kN) to the bearing, Fig. 6-right;

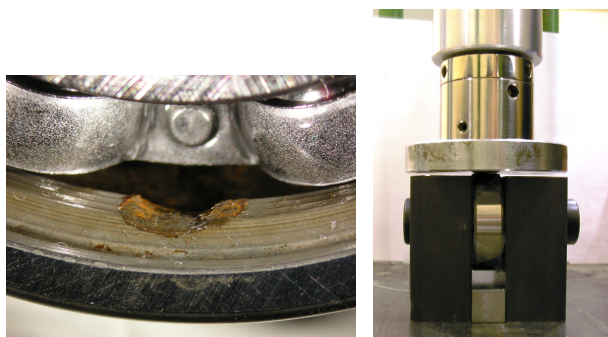


Fig. 6. Micrography of the chemically etched outer race defect (left). Photo of the hydraulic press employed to impart bearing brinelling damage (right).

The physical quantities monitored are: the radial vibration of the motor, the stator currents fed to the machine, the radial force exerted by the pneumatic cylinder and the load torque at the motor shaft. The vibration of the motor is measured by means of a mono-axial accelerometer placed on the frame of the test rig (sensitivity: 10.28 mV/g). The currents are measured by means of LEM LTSR 6-NP closed loop Hall current transducers (nominal current: 6 Arms; output voltage: 104,16 mV/A, accuracy: $\pm 0,2\%$) and the pressure by mean of a pressure sensor (output voltage: 0–10 V; measurement range: 0–10 bar, accuracy: $\pm 0,5\%$). The torque is measured by a torque meter mounted between the motor and the brake shafts (maximum torque: 20 Nm, linearity: $\pm 0,2\%$ of full scale).

VI. DESIGN OF EXPERIMENT

In an experiment, the relation between an output of the system and a given input is not straightforward. The output could be influenced by other initial conditions, machine parameters or the way the researcher had set up the experiment. The DOE approach fixes some procedures in order to minimize the influence of parameters other than the selected inputs, and proposes statistical tools to determine the significance of dependencies between the input and output of the system [37].

In this paper, the design of experiment for each test set consists of three independent factors with two levels each: the value of radial load, the load torque and the type of damage on the front bearing. Table V summarizes the factors and levels used in the first and second test run.

The output parameters, as described in the previous section, are the two scalar quantities defined as:

- The maximum amplitude of the auto power spectrum for the vibration signal filtered in the range [50Hz - 80Hz];

TABLE V
FACTORS AND LEVELS OF THE INDEPENDENT VARIABLES USED IN THE DESIGN OF EXPERIMENT (DOE).

First test set			
Factors:	Radial load	Load torque	Bearing status
Level 1	3 bar / 590 N	50%	healthy
Level 2	6 bar / 1180 N	100%	Outer race
Second test set			
Factors:	Radial load	Load torque	Bearing status
Level 1	3 bar / 590 N	50%	healthy
Level 2	6 bar / 1180 N	100%	Brinelling

- The RMS value of the residual current signal, i.e. once the 50 Hz and harmonics have been filtered out.

Two test set were performed in the laboratory trial, one employing a bearing with a localized fault on the outer race, the other employing a bearing with artificial brinelling. The resulting full factorial experimental plans consist of 8 randomized tests each, which are not replicated. The statistical analysis software Minitab was used to lay out the randomized test plan and to perform the analysis of variance (ANOVA) on the results. The levels of the independent variables were normalized: torque was normalized to the rated torque of the machine, radial load was normalized to the maximum value obtainable, while the fault is modeled as a binary variable (healthy = 0, faulty = 1).

VII. EXPERIMENTAL RESULTS

The test runs were performed according to the DOE and the physical quantities defined in Section V were acquired using 24 Bit, 51.2 kS/s data acquisition modules: for each test run, a 10 s length file was recorded for post processing and analysis. Figure 7 shows a comparison of the time signal of the vibration signal, in case of healthy and faulty front bearing. Figure 8 shows a comparison of the auto power spectrum of the vibration signal, in case of healthy and faulty front bearing. Figure 9 shows the effect of notch filtering on the FFT spectra of the healthy MUT current signal. The sidebands already present are due to the intrinsic unbalance of the electric machine caused by manufacturing tolerances. Figure 10 shows - on the same picture - a comparison of the spectrum of the current signal, in case of healthy and faulty front bearing (localized defect on the outer race). For uniformity of presentation, both the faulty and the healthy case shown are for a machine operated at rated output torque and 6 bar pressure on the radial load cylinder.

Since in a deep groove ball bearing the impact forces due to the bearing fault act mainly along a radial direction, it is reasonable to expect the torque ripple due to the bearing fault to be dependent upon radial load, but to be independent of the torque transmitted by the shaft. From preliminary observations on the radial vibration signals, no significant difference was observed between the test run with the MUT operating at no torsional load and at rated-torque: if the fault is present, fault signature is evident regardless of output torque.

Subsequently, currents and vibration signals were processed as described in Section IV to perform ANOVA on the results.

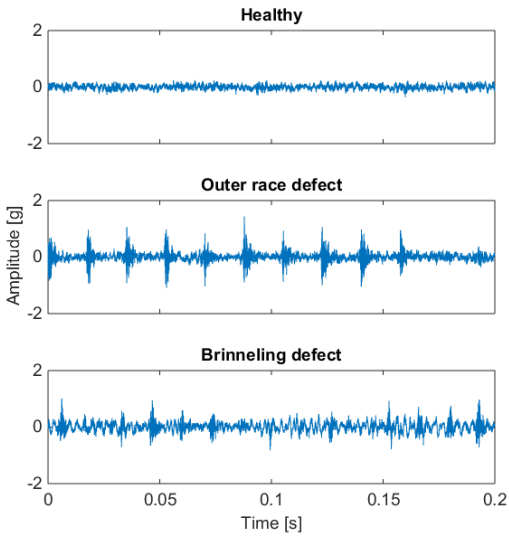


Fig. 7. Time domain signal of machine vibration operated at rated output torque and 6 bar pressure on the radial load cylinder: healthy bearing (upper), faulty bearing with single defect on the outer race (middle), faulty bearing with simulated brinneling (lower).

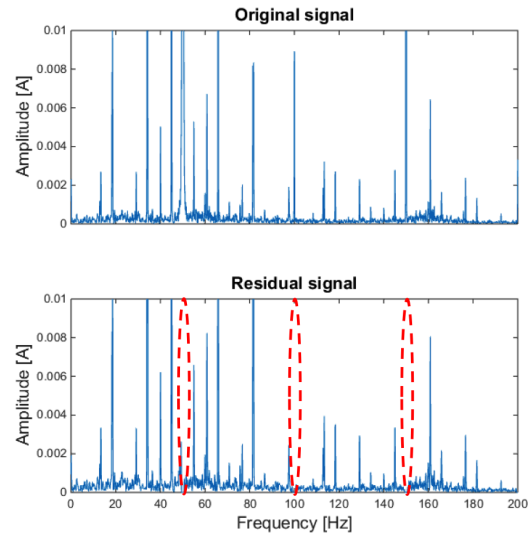


Fig. 9. Effect of notch filtering on the FFT spectra of the healthy MUT current signal operated at rated output torque and 6 bar pressure on the radial load cylinder: original signal (upper plot), residual signal after notch filtering of supply frequency harmonics (lower plot).

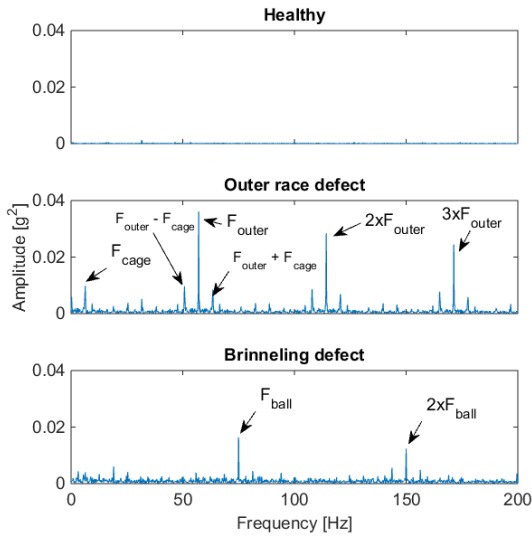


Fig. 8. Auto power spectrum of the vibration signal of the machine operated at rated output torque and 6 bar pressure on the radial load cylinder: healthy bearing (upper), faulty bearing (lower). The main components of the outer race fault frequency and its harmonics are side-banded with the periodicity of the cage.

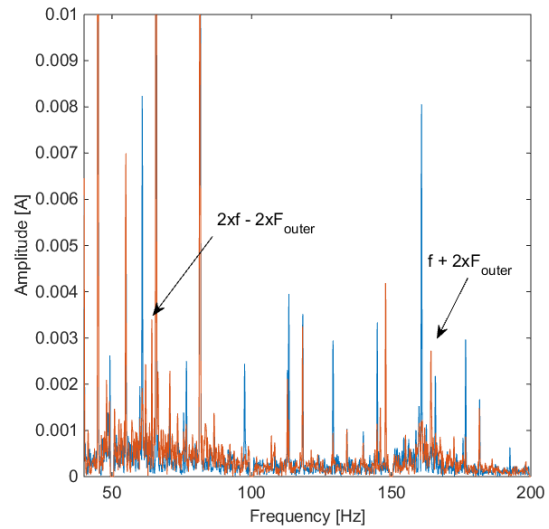


Fig. 10. Comparison of FFT spectra of the notch-filtered current signal of the MUT operated at rated output torque and 6 bar pressure on the radial load cylinder: healthy bearing (blue), faulty bearing with localized outer race defect (red).

Table VI shows a subset of values of the scalar fault indicators normalized to the healthy case, for the machine operated at rated torque and with 6 bar pressure on the radial load cylinder.

Useful for statistical analysis of multivariate problems and systems, ANOVA calculates the variance (standard deviation) of a response considering a specific variable and the global variance of the responses. The ratio between these two variances is called the F-Test value. In a stochastic (random) process F-value is equals to one, meaning that the considered variable has no effect on the response, i.e. it cannot be

distinguished from experimental noise or numerical error. Conversely the larger the F-Test value the more the variable influences the process. There are a number of approaches to represent the results graphically to demonstrate the effects of the variables on the system outputs. One of the most popular is the normal plot, used to estimate whether a certain set of data follows a Gaussian distribution or not. If the data approximates a straight line the phenomenon is statistically "normal" i.e. follows a stochastic law. The variables affecting the system response will then fall outside the normal distribution line, thus their effect cannot be ascribed to a stochastic process.

TABLE VI
SCALAR FAULT INDICATORS NORMALIZED TO HEALTHY CASE.

Indicator:	Healthy	Outer race	Brinnelling
Current	1	2	1.9
Vibration	1	25.6	11.1

The greater the deviation of the point from the normal line the larger the confidence interval (i.e. the probability that the variables are significant is higher). The half normal plot, used in this paper is interpreted in the same way as the normal plot but allows absolute values of the effects to be considered. The analysis was performed on the two system response described in Section IV: Figures 11 and 13 together with 12 and 14 show the half-normal probability plots from an ANOVA of vibration and current signals fault indicator respectively in case of the first (single point defect) and the second (brinnelling) test runs.

The ANOVA highlights the effects that significantly influence a physical phenomenon by comparing these effects of the output variable with a stochastic effect. This is obtained by comparing the results coming from the several levels of the selected experimental variable, driven by the stochastic experimental error. These values represent the probability that the effect of the variable is significant.

Half normal plots show the magnitude of the experiment's effects ordered in increasing magnitude along the x-axis. The effect for a factor is the difference of the average response variable over "high" factor levels minus the average response over the "low" factor levels. As said before, half normal plot show the distribution of the abs(X) with X having a normal distribution with mean zero. The points comprising factors with small and/or insignificant effects on the response will describe (roughly) a straight line on the plot. The points for factors with a 'large' and thus significant effects will visually fall off of the straight line described by the insignificant factors. A line through the insignificant factors helps to graphically delineate the difference between significant and insignificant factors. To visually interpret half normal plots: selecting the factor points which lie reasonably off of the line describing insignificant factors is an easy graphical way to identify important factors and start the process of optimizing the model.

Further details and additional statistical information on the half normal plot construction can be found in [38] and [39].

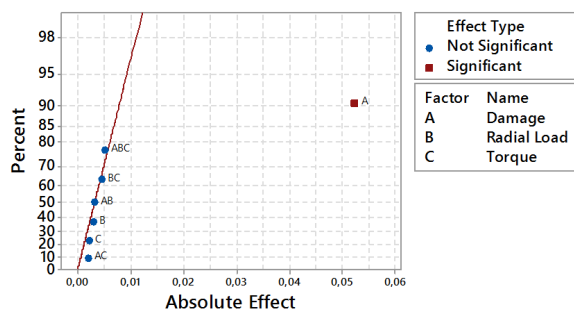


Fig. 11. Test set 1 (single point defect on outer race): Half normal plot of the scalar vibration fault indicator.

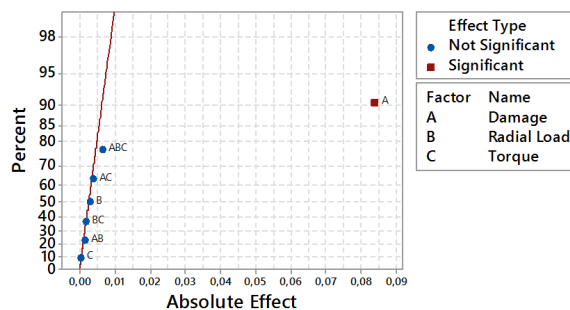


Fig. 12. Test set 1 (single point defect on outer race): Half normal plot of the scalar current fault indicator.

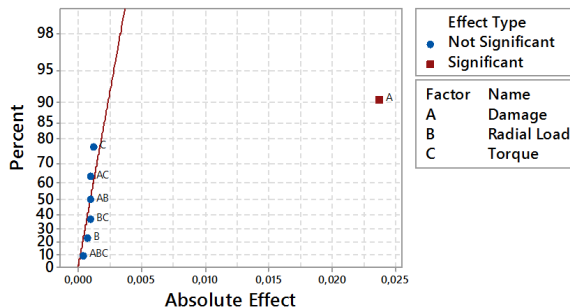


Fig. 13. Test set 2 (brinnelling defect): Half normal plot of the scalar vibration fault indicator.

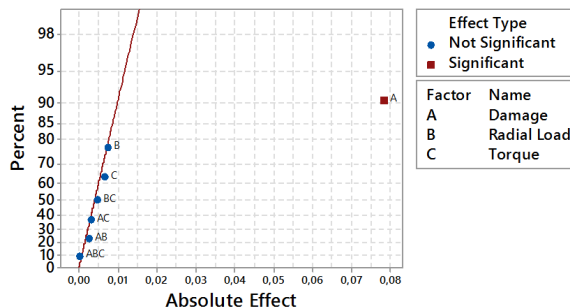


Fig. 14. Test set 2 (brinnelling defect): Half normal plot of the scalar current fault indicator.

Concerning the first test set on a single point defect on the outer race, Fig. 11 shows the half normal plot of the vibration fault indicator: as it can be seen, only the effect of the fault presence is significant, while load torque and radial load and their interactions have negligible effect. Figure 12 shows the half normal plot of the current fault indicator: in this case too the response is dominated only by the fault presence. Concerning the second test set on a simulated brinnelling fault Fig. 13 shows the half normal plot of the vibration fault indicator: as it can be seen, only the effect of the fault presence is significant, while load torque and radial load and their interactions have negligible effect. Figure 14 shows the half normal plot of the current fault indicator: in this case too the response is dominated only by the fault presence.

As mentioned in section II, the presence of radial load could lead to false positive fault detection due to the cyclic variation of the load, which is modulated by the passage of the revolving elements of the bearing. In order to investigate

this effect, further analysis has been done on a subset of the data available. Focusing on the healthy case only, Figs. 15 and 16 show the effects of the torque and load for the vibration and current signals respectively. In both cases the results suggest that the radial load has a negligible effect on the fault descriptors parameters. It is worth pointing out that with the present test setup, the maximum pressure in the pneumatic cylinder (6 bar) results in a radial loading force that is 1/6 of the maximum permissible static force provided by the bearing’s manufacturer. This represents a normal working condition: much higher values of load could cause an increase of the importance of radial load factor, but would result in reduced lifetime of the bearing and not typical of practical applications in everyday use.

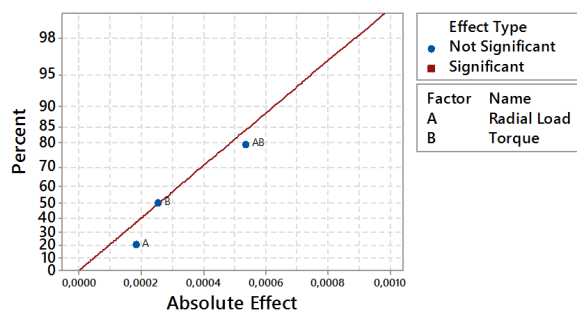


Fig. 15. Half normal plot of the scalar vibration fault indicator, healthy case subset.

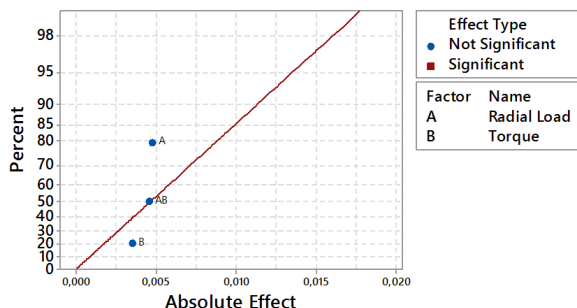


Fig. 16. Half normal plot of the scalar current fault indicator, healthy case subset.

VIII. CONCLUSION

This paper investigated the influence of external radial loads applied to the output shaft on bearing fault detection. The assessment was carried out experimentally, by applying a DOE approach to fault detection based on two scalar indicators for vibration and current signals respectively. A dedicated test setup was developed, comprising an extension shaft mounted on a sliding crosshead that allows to monitor vibration and current signals on a machine operating under different amount of radial load on the output shaft. The DOE approach was applied to a laboratory trial comprising two test sets with different faults on the machine’s bearing: a localized defect on the outer race and an artificial brinneling fault. The salient results are summarized in the following:

- The chosen scalar fault indicators allowed to positively identify the fault case with respect to the healthy one.
- For both test sets, only the effect of the fault presence is significant. This indicates a fair robustness of the chosen scalar fault indicators under different operating conditions and in case of different faults.
- Output torque, radial load and their interactions have negligible effect on both scalar fault indicators.
- Even in case of healthy bearing, the effect of radial load has no relevant effect on the vibration and current signals. The occurrence of false positive fault detection due to radial load is avoided.

The dedicated test rig developed in the present paper allows to independently apply radial and torque load on the machine’s shaft end. By using more elaborate DOE, it will allow to further investigate the influence of other factors and their interactions: e.g. the influence of operating speed, the influence of number of pole-pairs for a given power size.

REFERENCES

- [1] S. Nandi, H. A. Toliyat, and X. Li, “Condition monitoring and fault diagnosis of electrical motors—a review,” *IEEE Transactions on Energy Conversion*, vol. 20, no. 4, pp. 719–729, Dec 2005.
- [2] A. Bellini, F. Filippetti, C. Tassoni, and G. A. Capolino, “Advances in diagnostic techniques for induction machines,” *IEEE Transactions on Industrial Electronics*, vol. 55, no. 12, pp. 4109–4126, Dec 2008.
- [3] A. Garcia-Perez, R. d. J. Romero-Troncoso, E. Cabal-Yepez, and R. A. Osornio-Rios, “The application of high-resolution spectral analysis for identifying multiple combined faults in induction motors,” *IEEE Transactions on Industrial Electronics*, vol. 58, no. 5, pp. 2002–2010, May 2011.
- [4] O. V. Thorsen and M. Dalva, “A survey of faults on induction motors in offshore oil industry, petrochemical industry, gas terminals, and oil refineries,” *IEEE Transactions on Industry Applications*, vol. 31, no. 5, pp. 1186–1196, Sep 1995.
- [5] A. H. Bonnett, “Root cause ac motor failure analysis with a focus on shaft failures,” *IEEE Transactions on Industry Applications*, vol. 36, no. 5, pp. 1435–1448, Sep 2000.
- [6] C. Bianchini, F. Immovilli, M. Cocconcelli, R. Rubini, and A. Bellini, “Fault detection of linear bearings in brushless ac linear motors by vibration analysis,” *IEEE Transactions on Industrial Electronics*, vol. 58, no. 5, pp. 1684–1694, May 2011.
- [7] F. I. G. Curcuro, M. Cocconcelli and R. Rubini, “On the detection of distributed roughness on ball bearings via stator current energy: Experimental results,” *Diagnostyka*, vol. 51, no. 3, pp. 17–21, 2009.
- [8] L. Frosini and E. Bassi, “Stator current and motor efficiency as indicators for different types of bearing faults in induction motors,” *IEEE Transactions on Industrial Electronics*, vol. 57, no. 1, pp. 244–251, Jan 2010.
- [9] R. Rubini and U. Meneghetti, “Application of the envelope and wavelet transform analysis for the diagnosis of incipient faults in ball bearings,” *Mechanical Systems and Signal Processing*, vol. 15, no. 2, pp. 287 – 302, 2001.
- [10] J. R. Stack, T. G. Habetler, and R. G. Harley, “Fault-signature modeling and detection of inner-race bearing faults,” *IEEE Transactions on Industry Applications*, vol. 42, no. 1, pp. 61–68, Jan 2006.
- [11] A. Ibrahim, M. E. Badaoui, F. Guillet, and W. Youssef, “Electrical signals analysis of an asynchronous motor for bearing fault detection,” in *IECON 2006 - 32nd Annual Conference on IEEE Industrial Electronics*, Nov 2006, pp. 4975–4980.
- [12] L. Sun and B. Xu, “An improvement of stator current based detection of bearing fault in induction motors,” in *Industry Applications Conference, 2007. 42nd IAS Annual Meeting. Conference Record of the 2007 IEEE*, Sept 2007, pp. 2277–2281.
- [13] M. Blodt, M. Chabert, J. Regnier, and J. Faucher, “Mechanical load fault detection in induction motors by stator current time-frequency analysis,” *IEEE Transactions on Industry Applications*, vol. 42, no. 6, pp. 1454–1463, Nov 2006.

- [14] F. Immovilli, C. Bianchini, M. Cocconcelli, A. Bellini, and R. Rubini, "Bearing fault model for induction motor with externally induced vibration," *IEEE Transactions on Industrial Electronics*, vol. 60, no. 8, pp. 3408–3418, Aug 2013.
- [15] S. Choi, B. Akin, M. M. Rahimian, and H. A. Toliyat, "Performance-oriented electric motors diagnostics in modern energy conversion systems," *IEEE Transactions on Industrial Electronics*, vol. 59, no. 2, pp. 1266–1277, Feb 2012.
- [16] I. P. Georgakopoulos, E. D. Mitronikas, and A. N. Safacas, "Detection of induction motor faults in inverter drives using inverter input current analysis," *IEEE Transactions on Industrial Electronics*, vol. 58, no. 9, pp. 4365–4373, Sept 2011.
- [17] V. Choqueuse, M. E. H. Benbouzid, Y. Amirat, and S. Turri, "Diagnosis of three-phase electrical machines using multidimensional demodulation techniques," *IEEE Transactions on Industrial Electronics*, vol. 59, no. 4, pp. 2014–2023, April 2012.
- [18] J. I. Taylor and D. W. Kirkland, *The Bearing Analysis Handbook*. Vibration Consultants, 2004.
- [19] R. A. Fisher, *The design of experiments*. Hafner Publishing Company, 1971.
- [20] J. R. Stack, T. G. Habetler, and R. G. Harley, "Fault classification and fault signature production for rolling element bearings in electric machines," *IEEE Transactions on Industry Applications*, vol. 40, no. 3, pp. 735–739, May 2004.
- [21] —, "Bearing fault detection via autoregressive stator current modeling," *IEEE Transactions on Industry Applications*, vol. 40, no. 3, pp. 740–747, May 2004.
- [22] M. Blodt, D. Bonacci, J. Regnier, M. Chabert, and J. Faucher, "On-line monitoring of mechanical faults in variable-speed induction motor drives using the wigner distribution," *IEEE Transactions on Industrial Electronics*, vol. 55, no. 2, pp. 522–533, Feb 2008.
- [23] C. M. Riley, B. K. Lin, T. G. Habetler, and R. R. Schoen, "A method for sensorless on-line vibration monitoring of induction machines," *IEEE Transactions on Industry Applications*, vol. 34, no. 6, pp. 1240–1245, Nov 1998.
- [24] M. Blodt, P. Granjon, B. Raison, and G. Rostaing, "Models for bearing damage detection in induction motors using stator current monitoring," *IEEE Transactions on Industrial Electronics*, vol. 55, no. 4, pp. 1813–1822, April 2008.
- [25] F. Immovilli, A. Bellini, R. Rubini, and C. Tassoni, "Diagnosis of bearing faults in induction machines by vibration or current signals: A critical comparison," *IEEE Transactions on Industry Applications*, vol. 46, no. 4, pp. 1350–1359, July 2010.
- [26] R. B. Randall, *Vibration based condition monitoring*. Wiley and sons, 2011.
- [27] *ISO 10816-1: Evaluation of machine vibration by measurements on non-rotating parts*. Interstate Council For Standardization, Metrology And Certification Std.
- [28] S. D. S. V. R. D. Almeida and L. Padovese, "New technique for evaluation of global vibration levels in rolling bearings," *Shock and Vibration*, vol. 9, no. 4-5, pp. 225–234, 2002.
- [29] R. B. Randall and J. Antoni, "Rolling element bearing diagnostics tutorial," *Mechanical Systems and Signal Processing*, vol. 25, no. 2, pp. 485 – 520, 2011.
- [30] J. Yu, "Local and nonlocal preserving projection for bearing defect classification and performance assessment," *IEEE Transactions on Industrial Electronics*, vol. 59, no. 5, pp. 2363–2376, May 2012.
- [31] J. R. Stack, R. G. Harley, and T. G. Habetler, "An amplitude modulation detector for fault diagnosis in rolling element bearings," *IEEE Transactions on Industrial Electronics*, vol. 51, no. 5, pp. 1097–1102, Oct 2004.
- [32] P. McFadden and J. Smith, "The vibration produced by multiple point defects in a rolling element bearing," *Journal of Sound and Vibration*, vol. 98, no. 2, pp. 263 – 273, 1985.
- [33] R. RANDALL, J. ANTONI, and S. CHOBSAARD, "The relationship between spectral correlation and envelope analysis in the diagnostics of bearing faults and other cyclostationary machine signals," *Mechanical Systems and Signal Processing*, vol. 15, no. 5, pp. 945 – 962, 2001.
- [34] J. Antoni, F. Bonnardot, A. Raad, and M. E. Badaoui, "Cyclostationary modelling of rotating machine vibration signals," *Mechanical Systems and Signal Processing*, vol. 18, no. 6, pp. 1285 – 1314, 2004.
- [35] W. Gardner and L. Franks, "Characterization of cyclostationary random signal processes," *IEEE Transactions on Information Theory*, vol. 21, no. 1, pp. 4–14, Jan 1975.
- [36] K. Shin and J. K. Hammond, *Fundamentals of Signal Processing for Sound and Vibration Engineers*. Wiley and sons, 2008.
- [37] D. C. Montgomery, *Design and Analysis of Experiments*. Wiley and sons, 2012.
- [38] D. Cuthbert, "Use of half-normal plots in interpreting factorial two-level experiments," *Technometrics*, vol. 1, no. 4, pp. 311 – 341, 1959.
- [39] M. J. Anderson and P. J. Whitcomb, *DOE Simplified: Practical Tools for Effective Experimentation, Second Edition*. Productivity Press, 2007.



Fabio Immovilli was born in Italy on March 11, 1981. He received the M.S. degree and the Ph.D. in Mechatronic Engineering at the University of Modena and Reggio Emilia in 2006 and 2011 respectively. In 2009 he was a Visiting Scholar at the Power Electronics, Machines and Control Group of the University of Nottingham, Nottingham, UK. In 2011 he joined the University of Modena and Reggio Emilia, Reggio Emilia, Italy, as a Research Fellow in Electric Converters, Machines and Drives at the Department of Sciences and Methods of Engineering. His research interests include electric machine diagnosis, power converters, machines for energy conversion from renewable energy sources and thermoacoustics. He holds two international industrial patent.



Marco Cocconcelli was born in Italy on November 9, 1977. He received the M.S. degree in mechanical engineering and the Ph.D. degree in applied mechanics from the University of Bologna, Bologna, Italy, in 2003 and 2007, respectively. In 2007 he joined the University of Modena and Reggio Emilia, Reggio Emilia, Italy. He is researcher in applied mechanics at the Department of Sciences and Methods of Engineering. His research interests include bearing and gear diagnostics, condition monitoring in stationary and non-stationary conditions. He is a member of the Italian Association of Theoretical and Applied Mechanics (AIMETA), the Italian branch of the International Federation for the Promotion of Mechanism and Machine Science (IFToMM-Italy) and the International Society of Condition Monitoring (ISCM). He holds one international patent.